Journal of Materials Chemistry B

Accepted Manuscript

ROYAL SOCIETY OF CHEMISTRY

www.rsc.org/materialsB

Cite this: DOI: 10.1039/c0xx00000x

www.rsc.org/xxxxxx

ARTICLE TYPE

Facile Synthesis of Dental Enamel-like Hydroxyapatite Nanorod Arrays via Hydrothermal Transformation of Hillebrandite Nanobelts

Xiaohong Wang,[a] Yao Sun[b] and Kaili Lin[b,*]

Received (in XXX, XXX) Xth XXXXXXXXX 20XX, Accepted Xth XXXXXXXXX 20XX

DOI: 10.1039/b000000x

So far, the strategies for the synthesis of biomimetic dental enamel-like hydroxyapatite [$Ca_{10}(PO_4)_6(OH)_2$, HAp] have attracted great interests due to the extremely high orientation of HAp crystals. In present study, a facile method via hydrothermal treatment of the hillebrandite [$Ca_2(SiO_3)(OH)_2$] nanobelts as hard-template in trisodium phosphate aqueous solutions was developed to synthesize the dental enamel-like HAp nanorod arrays, in the absence of any proteins, surfactants, organic solvents or organic molecule directing reagents. The morphology observations demonstrated that the highly oriented HAp arrays were constructed by uniform nanorods in parallel to each other along the c-axis. A possible hard-template transformation mechanism based on the crystal structure and morphology of the hillebrandite nanobelts was proposed.

1 Introduction

As the main mineral component of vertebral skeleton, hydroxyapatite [$Ca_{10}(PO_4)_6(OH)_2$, HAp] is widely applied for medical and dental applications due to its excellent biocompatibility and osteo-conductivity.[1-6] The mineralized substance in skeleton possesses the distinct characters of highly orientated HAp arrays on nanoscale level and the arrays further woven into intricate architectures on the microscale level, which contributes to the excellent mechanical properties of the natural bones and teeth especially for high fracture resistance.[1,7] This unique hierarchical structure also plays a critical role in the protection and repairing of human teeth.[8] It is well known that the mature enamel is scarcely self-repaired when damaged.[1,9] Currently, setting the restorative materials on the defect sites in enamel is considered as the feasible method in enamel repairing. The studies suggested that the HAp materials with enamel-like structure might possess better affinity to the natural dental enamel comparing with the randomly oriented HAp materials and other kinds of materials including metals and resins.[1,10,11] Furthermore, the HAp is widely used as an absorbent in liquid chromatography due to its high absorption capacity with respect to proteins. It is well known that the different kinds of proteins are absorbed on different plane of HAp crystals as a manner that is related to the functional groups of the protein.[12,13] Therefore, the HAp materials with distinct crystal orientations might facilitate the preferential separation of different kinds of proteins.

Thus, the synthesis of HAp materials with enamel-like structure has been attracting great interests in biomaterial and biomedical fields. Many strategies have been developed to synthesize the enamel-like HAp. It is considered that the self-assembly of extracellular molecules plays a critical role in enamel and bone mineralization.[14,15] In which, as the abundant extracellular matrixes of enamel and bone, the amelogenin and collagen are the main factor in controlling the growth of apatite crystals in enamel and bone with well-organized and elongated manner. Fan et al.[16] proved that the appropriate concentrations of amelogenin promoted the oriented bundle formation of needle-like HAp crystals. Besides, using surfactants, ligands and organic solvents as the templates to direct the orientation of HAp crystals is another approach. The partially oriented HAp nanoclusters were achieved by Yang et al.[17] via refluxing method using the surfactant of potassium polyoxyethylene laurylether phosphate (MAEPK) as template. Due to the charge complement and the long organic chains of MAEPK, the HAp crystals nucleated on and grow oriented along the chain of MAEPK. The highly oriented organization of HAp nanorods could be achieved using mixed nonionic surfactants of P123 and tween-60 as the directing template.[18] Moreover, the hydrothermal method is considered as one of the most effective methods to control the morphologies and architectures of the HAp materials due to its capability to induce the nucleation and oriented growth of HAp crystals under hydrothermal condition.[2,19-24] Chen et al.[25] synthesized HAp powders with enamel-like microstructure using EDTA as ligand via hydrothermal treatment of 0.25 M EDTA-Ca-Na_2, 0.15 M $NaH_2PO_4 \cdot H_2O$ and 0.05 M NaF at 121 °C. Chen et al. reported a solvothermal method for the preparation of HAp oriented arrays using calcium acetylacetonate and creatine phosphate disodium salt tetrahydrate in mixed solvents of N,N-dimethylformamide (DMF) and water at 160 °C. In which, the creatine phosphate disodium salt tetrahydrate acted as an organic phosphorus source and a soft template for the formation of HAp oriented arrays.[26] The HAp nanowire/nanotube ordered arrays were obtained by hydrothermal treatment of the $CaCl_2$ and $NaH_2PO_4 \cdot H_2O$ in ternary solvents of water, ethylene glycol (EG) and N,N-dimethylformamide (DMF).[27] The synthesis of self-organized HAp nanorod arrays was reported by Chen et al.[28] through a

process of oriented attachment during hydrothermal treatment of the $CaCl_2$ and H_3PO_4, using dodecylamine as the ordered organic template.

However, the use of the additional additives in the preparation processes might limit their applications. For example, the utilizations of surfactants, macromolecules and organic solvents as structure-directing reagents might cause unnecessary biological effects, such as cytotoxicity. In addition, the usages of large amount of surfactants and organic solvents were harmful to health and environment.[24,26] Furthermore, the protein directing approach and the using of organic phosphate as phosphorus source and template can regulate the orientation of the crystals, but it is usually difficult to obtain the products in large-scale at low cost. Up to now, it is still a great challenge to facilely synthesize the enamel-like HAp materials.

Herein, a novel strategy was developed to synthesize the biomimetic HAp with enamel-like structures via direct hydrothermal transformation of the nanobelt-like hillebrandite $[Ca_2(SiO_3)(OH)_2]$ precursors in trisodium phosphate solution. This method did not use any surfactants, organic solvents or template-directing reagents, which effectively avoided the procedure and cost for their removal from the product.

2 Materials and methods

The biomimetic HAp with enamel-like structures were hydrothermally transformed from hillebrandite nanobelts in Na_3PO_4 aqueous solution without using any structure-directing reagents and organic solvents. Analytical grade reagents (Shanghai Chemical Co., Ltd., P.R. China) without further purification were used in present study.

2.1 Synthesis of hillebrandite $[Ca_2(SiO_3)(OH)_2]$ nanobelts

The hillebrandite $[Ca_2(SiO_3)(OH)_2]$ nanobelts were synthesized via hydrothermal method according to previous study.[29] Briefly, a solution was prepared by dissolving $Na_2SiO_3{\cdot}9H_2O$ (1.144 g) and NaOH (0.644 g) in deionized water (100 mL). Then the 40 mL of 0.20 M $Ca(NO_3)_2$ aqueous solution was quickly injected into the above Na_2SiO_3 aqueous solution to form a white suspension under vigorously magnetic stirring at room temperature. After completely addition, the suspension was transferred into the Teflon-lined stainless-steel autoclaves and heated at 200 °C for 24 h, followed by cooling down to room temperature naturally. After the hydrothermal treatment, the suspension was filtrated and washed with distilled water and anhydrous ethanol for three times, respectively. Finally, the obtained $Ca_2(SiO_3)(OH)_2$ nanobelts were dried at 120 °C for 24 h.

2.2 Hydrothermal transformation of the hillebrandite nanobelts into HAp with dental enamel-like structure

The synthetic hillebrandite nanobelts were used as the hard-template to synthesize the HAp with enamel-like structure. For hydrothermal process, the 1 g hillebrandite nanobelts were mixed with the 85 mL Na_3PO_4 (0.2 M) aqueous solution. Then the mixtures were transferred into 100 mL stainless steel autoclaves. The mixtures were heated at 150 °C for 0.5-24 h, followed by cooling to room temperature naturally. After the hydrothermal treatment, the reaction mixture was filtrated and washed with distilled water and anhydrous ethanol for three times, respectively. The obtained products were dried at 180 °C for 24 h for further characterization.

2.3 Characterization of the hard-template and the dental enamel-like HAp products

Both of the synthetic hard-template and the final HAp products were characterized by X-ray diffraction (XRD: D/max 2550V, Rigaku, Japan) with mono-chromated CuKα radiation, and Fourier transform infrared spectroscopy (FTIR: Nicolet Co., USA). The morphology and size of the synthetic hard-template and HAp were characterized by field emission transmission electron microscopy (FETEM: JEM-2100F, JEOL, Japan). The surface morphology and the thickness of the hard-template and the final HAp products were determined by field emission scanning electron microscopy (FESEM: JSM-6700F, JEOL, Japan). The chemical compositions of the HAp products were characterized by EDS mapping analysis technology (Oxford instruments). The surface area and nitrogen sorption isotherm were measured on a Micrometitics Tristar 3000 system.

3 Results and discussion

Fig. 1 shows the XRD patterns of the synthetic hard-template and the products after hydrothermal reaction of the hard-template in Na_3PO_4 aqueous solution at 150 °C for different periods. The synthetic hard-template (Fig. 1A) could be identified as pure hillebrandite phase (JCPDS card: No. 42-0538). The HAp phase (JCPDS card: No. 09-0432) appeared after hydrothermal reaction of the hillebrandite in Na_3PO_4 aqueous solution at 150 °C for 0.5 h (Fig. 1B). With the increase of the hydrothermal time to 2 h, the intensity of the most diffraction peaks for hillebrandite decreased apparently, while those for HAp increased improved remarkably (Fig. 1C). Further increasing the hydrothermal reaction time to 24 h, the diffraction peaks for hillebrandite disappeared completely, suggesting that the hard-templates have been completely transformed into the HAp products. In addition, the sharp peaks in the XRD pattern indicated that the synthetic HAp product transformed from hillebrandite template was well crystallized, which was attributed to the hydrothermal reaction in the synthetic process (Fig. 1D).

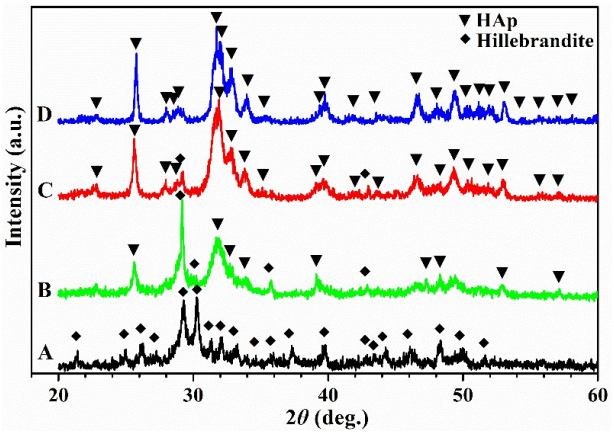

Fig. 1 XRD patterns of the synthetic hard-template (A) and the products after hydrothermal reaction of the hard-template in Na_3PO_4 aqueous solution at 150 °C for 0.5 h (B), 2 h (C) and 24 h (D).

The morphology observation result shows that the synthetic

hillebrandite were in belt-like shape with width of 0.4-1.5 μm and length up to 30 μm (Fig. 2A). The discrete SAED spots revealed that the synthetic hillebrandite nanobelts were well-crystallized single crystals. After hydrothermal reaction of the hillebrandite nanobelts in Na_3PO_4 aqueous solution at 150 °C for 0.5 h, the splitting phenomenon within the nanobelts along strip direction could be observed (Fig. 2B). Increasing the hydrothermal time to 2 h, the belt-like hard-templates completely disappeared and transformed into the biomimetic dental enamel-like nanorod arrays. The diameter of the nanorods was around 8-15 nm and the length was up to 60 nm (Fig. 2C). The morphology of the oriented nanorod arrays was maintained with further increasing of the hydrothermal time to 24 h, while the size of the nanorods grew wider and longer at the expense of smaller crystals with the increase of the reaction time.[24] The diameter and length of the oriented nanorods in final products were 10-20 nm and 100-200 nm, respectively (Fig. 2D), which were close to those of human enamel in sizes (a cross section of 33-65 nm and a length of 100-1000 nm along the c-axis.[30] According to the XRD characterization results (Fig. 1), the obtained oriented nanorods transformed from hillebrandite nanobelts was HAp phase. Further study of the synthetic nanorods by SAED showed the distinct diffraction rings with some bright points as shown in Fig. 2C-D. These points could be ascribed to (002) and (300) of HAp,[30] which the former further indicated that the synthetic HAp nanocrystals were well-aligned along c-axis and formed into bigger building units on microscale level.

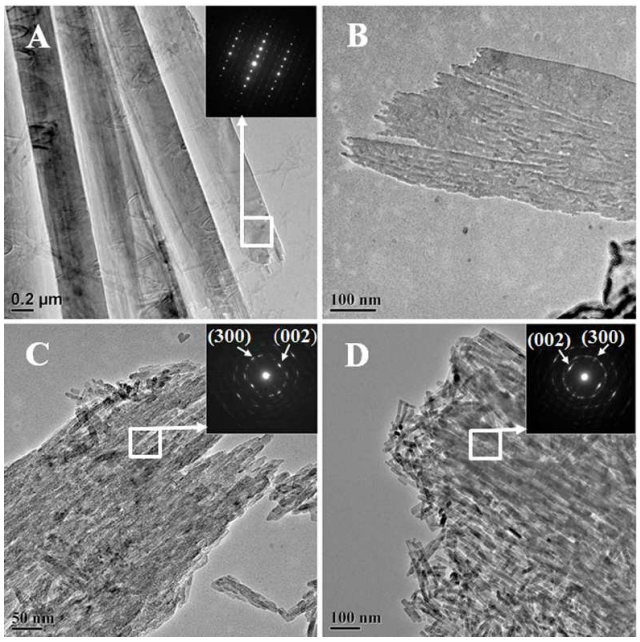

Fig. 2. FETEM images of the hard-template of hillebrandite (A), and the obtained products after hydrothermal treatment of the hillebrandite in Na_3PO_4 aqueous solution at 150 °C for 0.5 h (B), 2 h (C) and 24 h (D), respectively. The figures inserted at the top-right corner are the selective-area electron diffraction (SAED) images of the synthetic HAp products.

The surface morphologies of the hard-template and the synthetic enamel-like HAp nanorod arrays were further observed by FESEM (Fig. 3). The result further confirmed that the hard-template of hillebrandite was belt-like shape with smooth surface and thickness of about 200 nm (Fig. 3A). As expected, the final products hydrothermally transformed from hillebrandite nanobelts were constructed by orientated HAp arrays on nanoscale level and the arrays further woven into belt-like three-dimensional architectures on microscale level with similar length and thickness to hillebrandite nanobelts. In addition, the size of the HAp nanorods was similar to that observed in FETEM test.

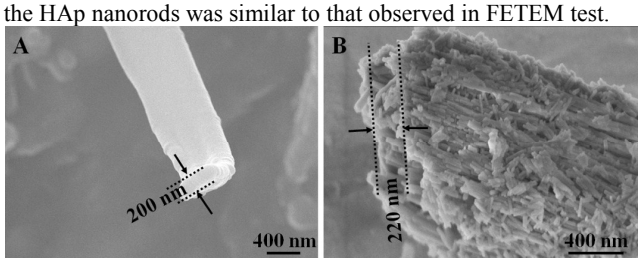

Fig. 3. FESEM images of the hard-template of hillebrandite (A), and the as-synthesized dental enamel-like HAp nanorod arrays via hydrothermal treatment of the hillebrandite at 150 °C for 24 h (B).

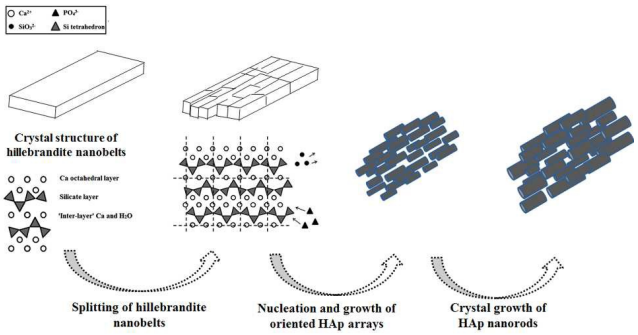

Fig. 4. Schematic illustration of the formation and morphology evolution of enamel-like HAp nanorod arrays in the whole synthetic process.

In present study, the dental enamel-like HAp nanorod arrays were successfully synthesized using hillebrandite nanobelts as hard-templates. On the basis of time-dependent experiments and the FETEM observations (Fig. 2-3), the evolution process of the oriented HAp arrays is summarized in Fig. 4, which may be due to the crystal structure and morphology of hillebrandite nanobelt itself. As a typical calcium silicate hydrate (CSH) material, the as-synthetized single-crystalline hillebrandite nanobelt is ordered phase with layered crystal structure. The layer consists of a central Ca-O part sandwiched between parallel silicate chains.[31,32] When hydrothermal treatment of the hillebrandite nanobelts in Na_3PO_4 aqueous solution, the sandwiched layers and silicate chains of the nanobelts were firstly split into smaller fragments in parallel, accompanying with the release of the Ca^{2+} and SiO_3^{2-} ions into the solutions. With the increase of the ion-release amount, the concentration of the Ca^{2+} and PO_4^{3-} reached over saturation and the HAp nucleated and grew on these fragmentations, resulting in the oriented rod-like products. During this process, the hillebrandite nanobelts played the roles of hard-template directing, calcium and silicon ion sources. In addition, the longer hydrothermal treatment increased the length of the nanorods due to their preferred orientation growth along the c-axis of HAp crystals.

The FTIR spectra of the hard-template of hillebrandite and the synthetic dental enamel-like HAp nanorod arrays are presented in Fig. 5. In spectrum for hillebrandite (Fig. 5A), the absorption bands of silicate group were evident. The intense bands at 857 and 1084 cm^{-1} were the bending stretch of Si-O-Si,

and the band at 465 cm^{-1} assigned to the Si-O-Si vibrational mode of bending. The peak at 713 cm^{-1} was the symmetric stretching vibration of Si-O-Si. The stretching vibration peak for OH^- appeared at 3430cm^{-1}.[33] While the wide adsorption at around 1490 cm^{-1} assigned to Ca-O stretching vibration.[34] The spectrum for the final products hydrothermally transformed from hillebrandite nanobelts is well in accord with the reported FTIR data of HAp (Fig. 5B). The peaks at 563, 603, 962, 1031 and 1093 cm^{-1} were the characteristic bands for PO_4^{3-}. The peak around 469 cm^{-1} was the overlap adsorption of PO_4^{3-} and Si-O. While the low intensities at 3568 and 631 cm^{-1} of the structural OH bands suggested that the PO_4 tetrahedra are replaced by SiO_4 tetrahedra in the HAp structure.[32,35] The bands at 1458 and 874 cm^{-1} were attributed to the carbonate group, which might come from the dissolved carbon dioxide in the hydrothermal solution. The weak peaks appeared at around 631 and 3568 cm^{-1} were the characteristic OH band of HAp, while the peaks around 1647 and 3462 cm^{-1} could be assigned to the bending mode of the absorbed water.[24] The FTIR results further confirmed that the as-synthesized products were silicon substituted HAp phase.

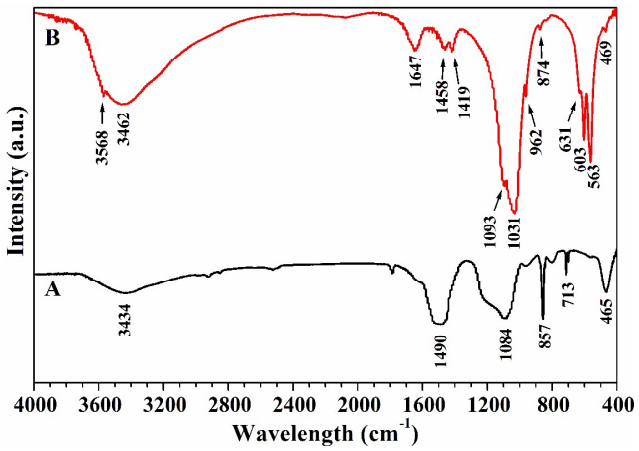

Fig. 5. FTIR spectra of the hard-template of hillebrandite (A), and the as-synthesized dental enamel-like HAp nanorod arrays via hydrothermal treatment of the hillebrandite at 150 °C for 24 h (B).

The EDS mapping technology was further applied to characterize the chemical compositions of the obtained enamel-like HAp nanorod arrays (Table 1). The results confirmed that the products was silicon-substituted HAp materials with silicon content of 0.33 wt.%. On the other hand, the Ca/P molar ratio of the obtained silicon substituted HAp nanorod arrays was slightly deviated from the stoichiometric HAp (Ca/P = 1.67).

Table 1. Chemical composition of the synthesized enamel-like HAp nanorod arrays via hydrothermal treatment of the hillebrandite at 150 °C for 24 h.

Element Concentrations of the synthesized enamel-like HAp nanorod arrays		
Si(IV) (wt.%)	Ca/P molar ratio	Ca/(P+Si) molar ratio
0.33	1.66	1.63

Moreover, the oriented arrays of the nanorods formed into bigger building units on microscale level in the synthetic dental enamel-like HAp materials might lead to higher specific surface area (S_{BET}) and formation of mesopores, which were confirmed by the nitrogen adsorption-desorption isotherm and the density functional theory (DFT) pore size distribution curve (Fig. 6). The S_{BET} of the dental enamel-like HAp nanorod arrays via hydrothermal treatment of the hillebrandite nanobelts in Na_3PO_4 aqueous solution at 150 °C for 24 h reached high value of 92.67 m^2/g, which was approximately 2-7 times as high as the HAp materials synthetized by traditionally chemical precipitation method,[36] chemical precipitation and then hydrothermal treatment approach,[20] and the hydrothermal homogeneous precipitation method,[20] etc. According to the International Union of Pure and Applied Chemistry, the data shown in Fig. 6 suggested that the synthetic dental enamel-like HAp nanorod arrays exhibit a type H4 hysteresis loop deriving from particle aggregates with slit-shaped pores in the range of 0.45~1.0 P/P0, which was typical of a mesoporous structure.[20,37] Calculated from the adsorption branches of the isotherms using the DFT method, the pore size mostly located in the range of 5-50 nm (Fig. 6). Based on the FETEM and FESEM observations, it can be concluded that the mesopores came from the free space within the bundles formed by HAp nanorod crystals at regular intervals.

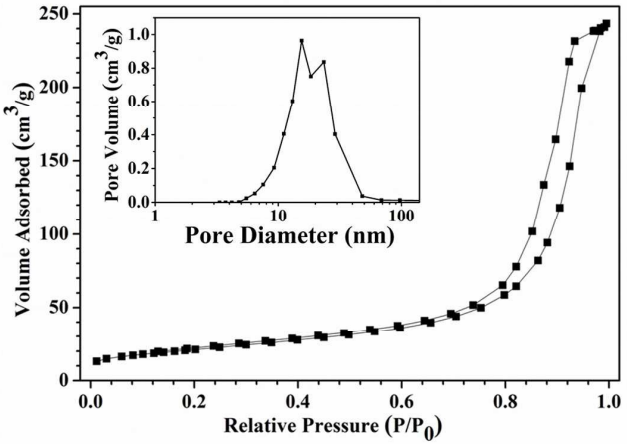

Fig. 6. The DFT pore size distribution of the synthetic dental enamel-like HAp nanorod arrays after hydrothermal treatment of the hillebrandite at 150 °C for 24 h.

It can be expected that the bulk HAp materials with enamel-like nanorod array structure might be obtained using bulk hard-templates as precursors. The future studies will be focused on the preparation of bulk materials in centimeter and then using as hard-templates to prepare the bulk HAp materials, which can be used for mechanical characterization and graft in hard tissue regeneration applications.

4 Conclusions

In summary, we developed a novel strategy to synthetize dental enamel-like hydroxyapatite (HAp) nanorod arrays via facilely hydrothermal treatment of the hillebrandite nanobelts in Na_3PO_4 aqueous solution. The hillebrandite nanobelts acted as the calcium ion source and a hard-template for the formation of HAp oriented arrays. The main advantage of this strategy is that the proteins or the environmentally unfriendly and unhealthy reagents are not needed, which avoids the procedures and cost for their removal in the final products. The synthetic HAp nanorod arrays with oriented structure show similarity in structure to the apatites presented in skeletons of human beings, and may be

potentially useful in biomedical fields.

Acknowledgments

The authors gratefully acknowledge the support of Natural Science Foundation of China (No.: 81171458), the Fund of the Science and Technology Commission of Shanghai Municipality (No.: 13NM1402102 & 15441905300), the Fund of Shanghai Municipal Commission of Health and Family Planning, and the Fundamental Research Funds for the Central Universities.

Notes and references

[a]*Laboratory of Oral Biomedical Science and Translational Medicine, Department of Endodontics, School of Stomatology, Tongji University, 399 Middle Yanchang Road, Shanghai 200072, China.*
[b]*Laboratory of Oral Biomedical Science and Translational Medicine, School of Stomatology, Tongji University, 399 Middle Yanchang Road, Shanghai 200072, China.*
Corresponding author: Tel: 86-21-56722215, Fax: 86-21-66524025. E-mail: lklecnu@aliyun.com (K. Lin).

1. Z. Zou, X. Liu, L. Chen, K. Lin and J. Chang, *J. Mater. Chem.* 2012, 22, 22637-22641.
2. K. Lin, C. Wu and J. Chang, *Acta Biomater.* 2014, 10, 4071-4102.
3. J. Xu, L. Liu, P. Munroe and Z. Xie, *J. Mater. Chem. B*, 2015, 3, 4082-4094.
4. J. Guan, B. Tian, S. Tang, Q. Ke, C. Zhang, Z. Zhu and Y. Guo, *J. Mater. Chem. B* 2015, 3, 1655-1666.
5. C. Zhao, L. Xia, D. Zhai, N. Zhang, J. Liu, B. Fang, J. Chang and K. Lin, *J. Mater. Chem. B* 2015, 3, 968-976.
6. P. Wang, L. Zhao, J. Liu, M. D. Weir, X. Zhou and H. H. K. Xu, *Bone Research* 2014, 2, 14017 (13 pages).
7. W. Xia, J. Lausmaa, P. Thomsen and H. Engqvist, *J. Biomed. Mater. Res*. 2012, 100B, 75-81.
8. L. Li, C. Mao, J. Wang, X. Xu, H. Pan, Y. Deng, X. Gu and R. Tang, *Adv. Mater.* 2011, 23, 4695-4701.
9. S. Busch, *Angew. Chem. Int. Ed.* 2004, 43, 1428-1431.
10. K. Yamagishi, K. Onuma, T. Suzuki, F. Okada, J. Tagami, M. Otsuki and P. Senawangse, *Nature* 2005, 433, 819.
11. S. Yang, H. He, L. Wang, X. Jia and H. Feng, *Chem. Commun.* 2011, 47, 10100-10102.
12. K. Inoue, K. Sassa, Y. Yokogawa, Y. Sakka, M. Okido and S Asai, *Mater. Trans*. 2003, 44, 1133-1137.
13. L. J. del Valle, O. Bertran, G. Chaves, G. Revilla-López, M. Rivas, M. T. Casas, J. Casanovas, P. Turon, J. Puiggalí and C. Alemán, *J. Mater. Chem. B* 2014,2, 6953-6966.
14. Q. Ruan and J. Moradian-Oldak, *J. Mater. Chem. B* 2015, 3, 3112-3129.
15. C. J. Newcomb, R. Bitton, Y. S. Velichko, M. L. Snead and S. I. Stupp, *small* 2012, 8, 2195-2202.
16. Y. Fan, Z. Sun and J. Moradian-Oldak, *Biomaterials* 2009, 30, 478-483.
17. S. Yang, J. Chen, Z. Wang, H. Zhang and Q. Zhang, *Mater. Lett.* 2013, 96, 177-180.
18. F. Ye, H. Guo and H. Zhan, *Nanotechnology* 2008, 19, 245605 (7pp).
19. Y. Wang, K. Lin, C. Wu, X. Liu and Jiang Chang, *J. Mater. Chem. B* 2015, 3, 65-71.
20. K. Lin, P. Liu, W. Zhang, L. Wei, Z. Zou, Y. Qian, Y. Shen and J Chang, *Chem. Eng. J.* 2013, 222, 49-59.
21. Y. Wang, C. Wu, K. Lin and J. Chang, *Chem. Asian. J.* 2013;8(5):990-996.
22. Y. Shen, J. Liu, K. Lin and W. Zhang, *Mater. Lett.* 2012, 70, 76-79.
23. K. Lin, Y. Zhou, Y. Zhou, H. Qu, F. Chen, Y. Zhu and J. Chang, *J. Mater. Chem.* 2011, 21, 16558-16565.
24. K. Lin, J. Chang, Y. Zhu, W. Wu, G. Cheng, Y. Zeng and M. Ruan, *Cryst. Growth Des.* 2009, 9, 177-181.
25. H. Chen, Z. Tang, J. Liu, K. Sun, S. Chang, M. C. Peters, J. F. Mansfield, A. Czajka-Jakubowska and B. H. Clarkson, *Adv. Mater.* 2006, 18, 1846-1851.
26. F. Chen, Y. Zhu, X. Zhao, B. Lu and J. Wu, *CrystEngComm*, 2013, 15, 4527-4531.
27. F. Chen, Y. J. Zhu, K. W. Wang and K. L. Zhao, *CrystEngComm* 2011,13, 1858-1863.
28. J. D. Chen, Y. J. Wang, K. Wei, S H. Zhang and X. T. Shi, *Biomaterials* 2007, 28, 2275-2280.
29. J. Wu and Y. Zhu, *Mater. Lett.* 2009, 63, 761-763.
30. J. Zhang, D. Jiang, J. Zhang, Q. Lin and Z. Huang, *Langmuir* 2010, 26, 2989-2994.
31. H. F. W. Taylor, *J. Am. Ceram. Soc.* 1986, **69**, 464-467.
32. K. Lin, J. Chang, X. Liu, L. Chen and Y. Zhou, *CrystEngComm* 2011, 13, 4850-4855.
33. Z. Gou, J. Chang, J. Gao and Z. Wang, *J. Eur. Ceram. Soc.* 2004, 24, 3491-3497.
34. M. A. Tantawy, M. R. Shatat, A. M. El-Roudi, M. A. Taher and M. Abd-El-Hamed, *Int. Scholarly Res. Notices* 2014, 873215 (10 pages).
35. S. R. Kim, J. H. Lee, Y. T. Kim, D. H. Riu, S. J. Jung, Y. J. Lee, S. C. Chung and Y. H. Kim, *Biomaterials*, 2003, 24, 1389-1398.
36. K. Lin, J. Pan, Y. Chen, R. Cheng and X. Xu, *J. Hazard. Mater.* 2009, 161, 231-240.
37. K.S.W. Sing, *Pure Appl. Chem.* 1982, 54, 2201-2218.

Graphical Abstract

The biomimetic dental enamel-like hydroxyapatite (HAp) nanorod arrays were facilely synthetized via hydrothermal treatment of the hillebrandite nanobelts as hard-template in trisodium phosphate aqueous solutions.